

# The production of $K^+K^-$ pairs in proton-proton collisions below the $\phi$ meson threshold

Q. J. Ye,<sup>1,2,\*</sup> M. Hartmann,<sup>2,†</sup> D. Chiladze,<sup>2,3</sup> S. Dymov,<sup>4,5</sup> A. Dzyuba,<sup>6</sup> H. Gao,<sup>1</sup>  
R. Gebel,<sup>2</sup> V. Hejny,<sup>2</sup> A. Kacharava,<sup>2</sup> B. Lorentz,<sup>2</sup> D. Mchedlishvili,<sup>2,3</sup> S. Merzliakov,<sup>2,5</sup>  
M. Mielke,<sup>7</sup> S. Mikirtychiants,<sup>2,6</sup> H. Ohm,<sup>2</sup> M. Papenbrock,<sup>7</sup> A. Polyanskiy,<sup>2,8</sup> V. Serdyuk,<sup>2,5</sup>  
H. J. Stein,<sup>2</sup> H. Ströher,<sup>2</sup> S. Trusov,<sup>9,10</sup> Yu. Valdau,<sup>2,11</sup> C. Wilkin,<sup>12</sup> and P. Wüstner<sup>13</sup>

<sup>1</sup>*Department of Physics and Triangle Universities Nuclear Laboratory, Duke University, Durham, NC 27708, USA*

<sup>2</sup>*Institut für Kernphysik and Jülich Centre for Hadron Physics,  
Forschungszentrum Jülich, D-52425 Jülich, Germany*

<sup>3</sup>*High Energy Physics Institute, Tbilisi State University, GE-0186 Tbilisi, Georgia*

<sup>4</sup>*Physikalisches Institut, Universität Erlangen-Nürnberg, D-91058 Erlangen, Germany*

<sup>5</sup>*Laboratory of Nuclear Problems, Joint Institute for Nuclear Research, RU-141980 Dubna, Russia*

<sup>6</sup>*High Energy Physics Department, Petersburg Nuclear Physics Institute, RU-188350 Gatchina, Russia*

<sup>7</sup>*Institut für Kernphysik, Universität Münster, D-48149 Münster, Germany*

<sup>8</sup>*Institute for Theoretical and Experimental Physics, RU-117218 Moscow, Russia*

<sup>9</sup>*Institut für Kern- und Hadronenphysik, Helmholtz-Zentrum Dresden-Rossendorf, D-01314 Dresden, Germany*

<sup>10</sup>*Skobeltsyn Institute of Nuclear Physics, Lomonosov Moscow State University, RU-119991 Moscow, Russia*

<sup>11</sup>*Helmholtz-Institut für Strahlen- und Kernphysik, Universität Bonn, D-53115 Bonn, Germany*

<sup>12</sup>*Physics and Astronomy Department, UCL, London WC1E 6BT, United Kingdom*

<sup>13</sup>*Zentralinstitut für Elektronik, Forschungszentrum Jülich, D-52425 Jülich, Germany*

(Dated: November 11, 2018)

The  $pp \rightarrow ppK^+K^-$  reaction was measured below the  $\phi$  threshold at a beam energy of 2.568 GeV using the COSY-ANKE magnetic spectrometer. By assuming that the four-body phase space is distorted only by the product of two-body final state interactions, fits to a variety of one-dimensional distributions permit the evaluation of differential and total cross sections. The shapes of the distributions in the  $Kp$  and  $Kpp$  invariant masses are reproduced only if the  $K^-p$  interaction is even stronger than that found at higher energy. The cusp effect in the  $K^+K^-$  distribution at the  $K^0\bar{K}^0$  threshold is much more clear and some evidence is also found for coupling between the  $K^-p$  and  $\bar{K}^0n$  channels. However, the energy dependence of the total cross section cannot be reproduced by considering only a simple product of such pair-wise final state interactions.

PACS numbers: 13.75.-n, 25.40.Ep, 13.75.Jz

## I. INTRODUCTION

The original motivation for the study of kaon-pair production in the  $pp \rightarrow ppK^+K^-$  reaction near threshold was the investigation of the structure of the scalar mesons  $a_0(980)$  or  $f_0(980)$  [1]. Such measurements were initially performed by the COSY-11 collaboration at several different excess energies below the  $\phi$ -meson production threshold [2–4]. However, their results showed that scalar meson production cannot in fact be the dominant driving mechanism in kaon pair production [3] and that the data can be explained without the explicit inclusion of the  $a_0/f_0$ . Furthermore, they showed that the  $K^-p$  and  $K^-pp$  invariant mass spectra were strongly distorted, presumably by the  $K^-p$  final state interaction (FSI) [4]. This was most apparent in the ratio of the differential cross sections in terms of the  $K^-p$  and  $K^+p$  invariant masses.

The  $pp \rightarrow ppK^+K^-$  reaction was also investigated

with higher statistics above the threshold for the production of the  $\phi$  meson, mainly with the aim of investigating the properties of that meson [5–8]. After removing the  $\phi$  contribution in the spectra, it was clear that the  $K^-p$  and  $K^-pp$  distributions in the non- $\phi$  data were both strongly influenced by the  $K^-p$  interaction [6, 8]. It has been suggested that this is connected with the production of the  $\Lambda(1405)$  excited hyperon [9], which might be treated as a  $\bar{K}N$  quasi-bound state with a width that overlaps the  $\bar{K}N$  threshold [10]. This idea was put on a quantitative footing by assuming that the  $\Lambda(1405)$  was formed through the decay  $N^* \rightarrow K^+\Lambda(1405)$  [11]. The strength and details of the  $\bar{K}N$  interaction are clearly important elements in the interpretation of possible kaon nuclear systems, such as the deeply bound  $K^-pp$  states [12].

In addition to the  $K^-p$  FSI, and one between the two protons, the data also showed an enhancement at low  $K^+K^-$  invariant masses with some possible structure at the  $K^0\bar{K}^0$  threshold [6–8]. Though the effects are small, they might be influenced by the  $a_0(980)$  or  $f_0(980)$  scalar mesons. However, the investigation of this region was hampered by the need to separate the non- $\phi$  from the  $\phi$  contribution and the fact that the data were spread over a very wide range of  $K^+K^-$  invariant masses. Measure-

\*Electronic address: qy4@phy.duke.edu

†Electronic address: m.hartmann@fz-juelich.de

ments below the  $\phi$  threshold can provide useful information on these interesting FSI effects without suffering the distortion of the  $\phi$  meson. However, the limited statistics in the low-energy COSY-11 data [2–4] are insufficient for detailed studies.

Previous measurements of the  $pp \rightarrow ppK^+K^-$  reaction were carried out at the COSY-ANKE magnetic spectrometer at  $\varepsilon = 51, 67, \text{ and } 108 \text{ MeV}$  [6, 8], where the  $\phi$  threshold is at  $\varepsilon = 32.1 \text{ MeV}$ . Here the excess energy is defined as  $\varepsilon = \sqrt{s} - 2(m_p + m_K)c^2$ , where  $\sqrt{s}$  is the total center-of-mass energy and  $m_p$  and  $m_K$  are the particle masses in the final state. Because of the limited acceptance of this spectrometer, an ansatz has to be made regarding the distribution of events over the four-body phase space in order to convert count rates into cross sections. This was done assuming that the distortions were the products of those present in the two-particle subsystems. All the ANKE non- $\phi$  data seemed to be consistent with an *effective* scattering length of  $a_{K^-p} = (0 + 1.5i) \text{ fm}$  with no obvious influence of an energy dependence associated with an effective range term. The dominance of the imaginary part is not unexpected because of the strong couplings to the  $\Sigma\pi$  and  $\Lambda\pi$  channels but, due to the presence of two other final-state particles, this parameter is not necessarily an intrinsic feature of the isolated  $K^-p$  system.

The ANKE measurements at three excess energies also showed some enhancement at low  $K^+K^-$  invariant masses but with at least a break of slope at the  $K^0\bar{K}^0$  threshold. A combined analysis of all the results in this region [7, 8] shows that the data can be understood in terms of a final state interaction involving both  $K^+K^-$  elastic scattering plus a contribution from the  $K^+K^- \rightleftharpoons K^0\bar{K}^0$  charge exchange. Although suggestive, the data are not sufficient to draw firm conclusions.

In this paper we present much more precise  $pp \rightarrow ppK^+K^-$  differential cross section data at a beam energy of  $T_p = 2.568 \text{ GeV}$  ( $\varepsilon = 23.9 \text{ MeV}$ ) obtained using the COSY-ANKE spectrometer. With high statistics on the reaction below the  $\phi$ -meson threshold, we could study the effects of the final state interactions in the  $K^-p$  and  $K^+K^-$  systems in greater details.

The paper is organized as follows. We first describe the experimental setup and data analysis in Sec II. Given that the procedures involved are similar to those employed at higher energies [6, 8], this can be quite brief. The fitting of the phenomenological parametrization to the raw  $pp \rightarrow ppK^+K^-$  data in order to make acceptance corrections is also described here. The resulting differential cross sections and total cross section for the  $pp \rightarrow ppK^+K^-$  reaction are presented in Sec III, followed by our conclusions in Sec IV.

## II. EXPERIMENT AND DATA ANALYSIS

The measurement of the  $pp \rightarrow ppK^+K^-$  reaction was performed at an internal target station of the Cooler Syn-

chrotron (COSY) of the Forschungszentrum Jülich [13]. The ANKE spectrometer [14, 15], which consists of three dipole magnets, registers positively and negatively charged ejectiles in the side detection systems, with the fast positively charged particles being detected in the forward detector. Particle identification relies on time-of-flight measurements [6, 15–17] from START and STOP counters, and momentum information obtained from the multiwire proportional chambers.

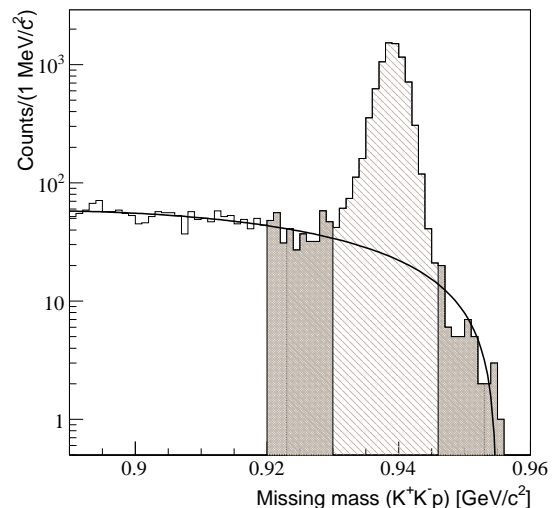


FIG. 1: The  $pK^+K^-$  missing-mass distribution in the  $pp \rightarrow pK^+K^-X$  reaction at  $T_p = 2.568 \text{ GeV}$ . The hatched histogram shows the cuts imposed for the selection of the non-detected proton. The solid line, which is a second-order polynomial fit, was used to estimate the background contribution under the proton peak.

In close-to-threshold production experiments, the total cross section changes very rapidly with small changes in the excess energy. The proton beam energy,  $T_p = 2.568 \text{ GeV}$ , was therefore determined very precisely through a careful monitoring of the Schottky spectra [18]. The resulting value of the excess energy with respect to the  $ppK^+K^-$  production threshold,  $\varepsilon = 23.9 \text{ MeV}$ , is well below the nominal  $\phi$  threshold. However it should be noted that this is an average value, since the beam energy decreases by up to  $4.6 \text{ MeV}$  through the course of a machine cycle due to the interaction with the target. This effect was also investigated in the simulation.

The experiment relied on a triple-coincidence, involving the observation of a  $K^+K^-$  pair in the side detectors and a fast proton in the forward detector. The  $pp \rightarrow ppK^+K^-$  reaction was then identified by requiring that the missing mass of the  $K^+K^-p$  system be consistent with that of a proton. In the analysis, a  $\pm 3\sigma$  ( $\sigma = 2 \text{ MeV}/c^2$ ) cut was applied on the missing-mass distribution of the selected  $K^+K^-p$  events, as shown in Fig. 1. The fraction of misidentified events inside the cut window around the proton mass was estimated to

be about 5%, which was subtracted from the peak using weighted data from the side bands, as parameterized by the solid line. Any ambiguity in this procedure, which is less than 3%, is one source of systematic uncertainty.

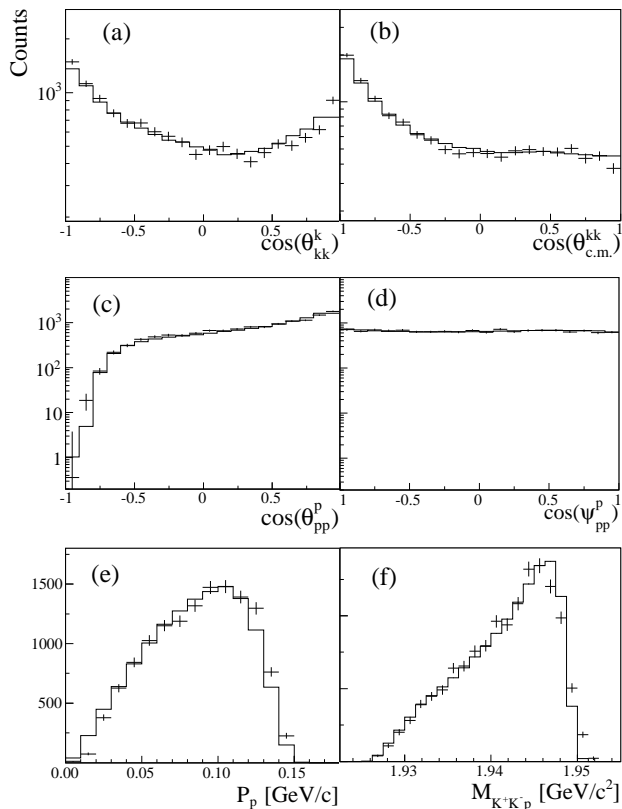


FIG. 2: Differential distributions of experimental (points) and simulated (histograms) yields for kaon pair production in the  $pp \rightarrow ppK^+K^-$  reaction at  $\varepsilon = 23.9$  MeV. Vertical bars represent the statistical uncertainties and horizontal ones the bin widths. The individual panels are (a) the cosine of the polar angle of the  $K^+$  in the  $K^+K^-$  reference frame, (b) the polar angle of the kaon pairs in the overall c.m. frame, (c) the polar angle of the emitted proton in the  $pp$  reference frame relative to the beam direction, (d) the polar angle of the proton in the  $pp$  reference frame relative to the direction of the kaon pair, (e) the proton momentum in the  $pp$  reference frame, and (f) the  $K^+K^-p$  invariant mass.

After identifying clean  $pp \rightarrow ppK^+K^-$  events in ANKE, acceptance corrections must be performed in order to evaluate differential cross sections. The simple ansatz used on data taken above the  $\phi$  meson production threshold tried to take into account the influence of final state interactions in the various two-particle subsystems [6, 8]. This ansatz, which is also the basis for the current simulation, assumes that the overall enhancement factor  $F$  is the product of enhancements in the  $pp$ ,  $K^+K^-$ , and  $K^-p$  systems:

$$F = F_{pp}(q_{pp}) \times F_{Kp}(q_{Kp_1}) \times F_{Kp}(q_{Kp_2}) \times F_{KK}(q_{KK}), \quad (1)$$

where  $q_{pp}$ ,  $q_{Kp_1}$ ,  $q_{Kp_2}$ , and  $q_{KK}$  are the magnitudes of the relative momenta in the  $pp$ , the two  $K^-p$ , and the  $K^+K^-$  system, respectively. It is believed that the  $K^+p$  interaction might be weakly repulsive and, if so, its neglect would be interpreted as extra attraction in the  $K^-p$  system. The FSI enhancement in the  $K^-p$  case was calculated in the scattering length approximation,  $F_{Kp}(q) \approx 1/|1 - iqa|^2$  and the best fit to the higher energy data [6, 8] was found with a purely imaginary effective scattering length,  $a_{K-p} \approx 1.5i$  fm. The proton-proton enhancement factor was derived from the Jost function [6, 8]. The enhancement factor in the  $K^+K^-$  system takes into account elastic  $K^+K^-$  scattering plus the charge-exchange  $K^+K^- \rightleftharpoons K^0\bar{K}^0$  [7].

The seven degrees of freedom required to describe the unpolarized  $ppK^+K^-$  final state were chosen to be four angles, the  $K^+K^-$  and  $K^+K^-p$  invariant masses, and the relative momentum of the protons in the  $pp$  system [6, 8]. Distributions in these seven variables were generated inside the ANKE acceptance and compared with the experimental data, some of which are shown in Fig. 2. The best fit to the data was achieved with  $a_{K-p} = (2.45 \pm 0.4)i$  fm, which is significantly larger in magnitude than the starting value of  $a_{K-p} = 1.5i$  fm. The uncertainty in the real part is large and strongly correlated with the imaginary part. To allow easy comparison with the analysis of the higher energy data [6, 8], the effective scattering length was taken to be purely imaginary.

The  $\bar{K}K$  scattering lengths for isospin-one and zero were taken as in our previous work [7] and the ratio of the  $I = 1$  and  $I = 0$  production amplitudes of  $s$ -wave  $K\bar{K}$  pairs was parameterized as  $Ce^{i\phi_c}$ . The best fit was obtained with  $C = 0.54 \pm 0.03$  and  $\phi_c = -112^\circ \pm 4^\circ$ , which are consistent with our earlier evaluation [7, 8] based on the above  $\phi$  threshold data. The resulting descriptions of the experimental data in Fig. 2 are very good and certainly sufficient for evaluating the acceptance corrections.

The luminosity needed in the analysis was determined with an overall systematic uncertainty of 9% by measuring  $pp$  elastic scattering in the forward detector [6]. This was checked by simultaneous studies of the beam current and Schottky spectra [18], which could fix the absolute luminosity with a systematic uncertainty of 6%. Within these uncertainties the two methods agreed but, in order to be coherent with our previous work, the luminosity extracted from the  $pp$  elastic scattering data was used in the final analysis.

### III. RESULTS

The differential cross section for the  $pp \rightarrow ppK^+K^-$  reaction at an excess energy  $\varepsilon = 23.9$  MeV is shown in Fig. 3 as a function of the  $K^+K^-$  invariant mass. Also shown are simulations based on a four-body phase space and this distorted by the final state interactions in the  $K^+K^-$ ,  $pp$ , and  $K^-p$  systems within the product ansatz

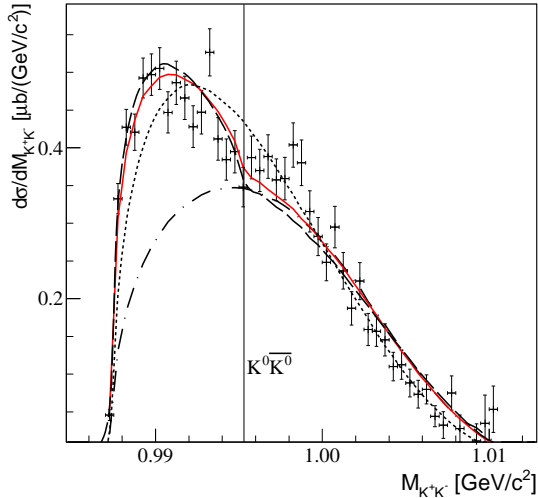


FIG. 3: (Color online) The  $pp \rightarrow ppK^+K^-$  differential cross section at  $\varepsilon = 23.9$  MeV as a function of the  $K^+K^-$  invariant mass. The dotted curve shows the four-body phase space simulation whereas the inclusion of the final state interactions through Eq. (1) gives the dashed curve for  $a_{K^-p} = 1.5i$  fm and the red solid curve  $a_{K^-p} = 2.45i$  fm. The dot-dashed curve was obtained by considering only the  $pp$  and  $K^-p$  final state interactions with  $a_{K^-p} = 2.45i$  fm.

of Eq. (1). This was done separately with effective scattering lengths of  $a_{K^-p} = 1.5i$  fm and  $a_{K^-p} = 2.45i$  fm.

The most striking features in the data are the strength near the  $K^+K^-$  threshold and the dip at  $M_{K^+K^-} \approx 0.995$  GeV/ $c^2$ , which corresponds precisely to the  $K^0\bar{K}^0$  production threshold [7]. This is compelling evidence for a cusp effect coming from the  $K^0\bar{K}^0 \rightleftharpoons K^+K^-$  transitions. To investigate this phenomenon in greater detail, the  $K^+K^-$  invariant mass distribution was divided by a simulation where only the final state interactions in the  $pp$  and  $K^-p$ , with  $a_{K^-p} = 2.45i$  fm, were considered. The best fit to the data shown in Fig. 4 is achieved with a contribution from the isospin-zero channel that is about three times stronger than the isospin-one. This finding is consistent with our earlier result [7]. The deviations apparent in Figs. 3 and 4 at high  $K^+K^-$  invariant masses might be connected with the approximations made in our coupled-channel model [7].

Previous analyses of the  $pp \rightarrow ppK^+K^-$  reaction at different excess energies [4, 6, 8, 19] have all shown a strong preference for low values of the  $K^-p$  and  $K^-pp$  invariant masses,  $M_{K^-p}$  and  $M_{K^-pp}$ . To study this further, we have evaluated differential cross sections as functions of these invariant masses and also the ratios:

$$R_{Kp} = \frac{d\sigma/dM_{K^-p}}{d\sigma/dM_{K^+p}},$$

$$R_{Kpp} = \frac{d\sigma/dM_{K^-pp}}{d\sigma/dM_{K^+pp}}. \quad (2)$$

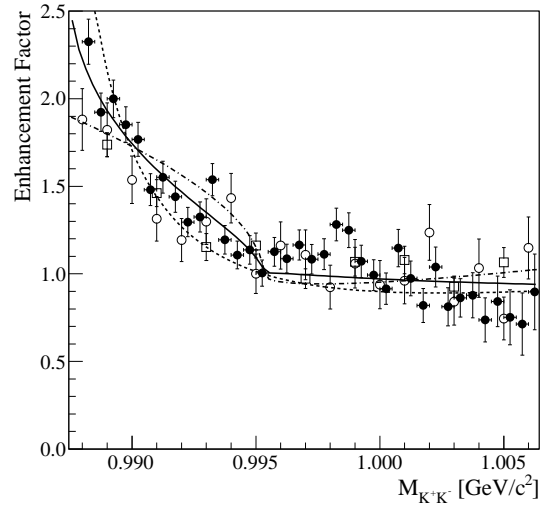


FIG. 4: Ratio of the measured  $pp \rightarrow ppK^+K^-$  differential cross section at  $\varepsilon = 23.9$  MeV as a function of the  $K^+K^-$  invariant mass to a simulation that includes only  $K^-p$  and  $pp$  final state interactions (shown by the dot-dashed curve in Fig. 3). In addition to the current data (solid circles), weighted averages of previous measurements (open squares and circles) are also presented. The solid curve represents the best fit in a model that includes elastic  $K^+K^-$  FSI and  $K^0\bar{K}^0 \rightleftharpoons K^+K^-$  charge-exchange [7]. The best fits neglecting charge exchange and including only this effect are shown by the dashed and dot-dashed curves, respectively.

The corresponding experimental data and simulations are shown in Figs. 5 and 6. Both  $R_{Kp}$  and  $R_{Kpp}$  display the very strong preferences for lower invariant masses seen in the earlier data. The low mass enhancements in Figs. 5c and 6c clearly indicate once again that the  $pp \rightarrow ppK^+K^-$  reaction cannot be dominated by the undistorted production of a single scalar resonance  $a_0$  or  $f_0$ . Within a four-body phase space simulation both ratios should be constant and equal to one and such a simulation also fails to describe the  $M_{Kp}$  and  $M_{Kpp}$  distributions. Whereas the inclusion of a  $K^-p$  FSI with an effective scattering length  $a_{K^-p} = 1.5i$  fm improves the situation, it overestimates the data in the high invariant mass regions for both  $R_{Kp}$  and  $R_{Kpp}$ . With the larger effective scattering length  $a_{K^-p} = 2.45i$  fm, these ratios, as well as the individual differential cross sections, can be well reproduced. Within the product ansatz of Eq. (1) the  $K^-p$  final state interaction effectively becomes stronger at lower excess energies. This illustrates the limitations of this simple ansatz to the complex four-body dynamics.

Although the  $K^-p$  elastic final state interaction describes well the vast bulk of the data shown in Figs. 5 and 6, it is interesting to note that there seems to be a small but significant deviation between the  $K^-p$  data and simulation in Fig. 5b at low invariant masses. Since the  $\bar{K}^0n$  threshold is at 1.437 GeV/ $c^2$ , this suggests that the data

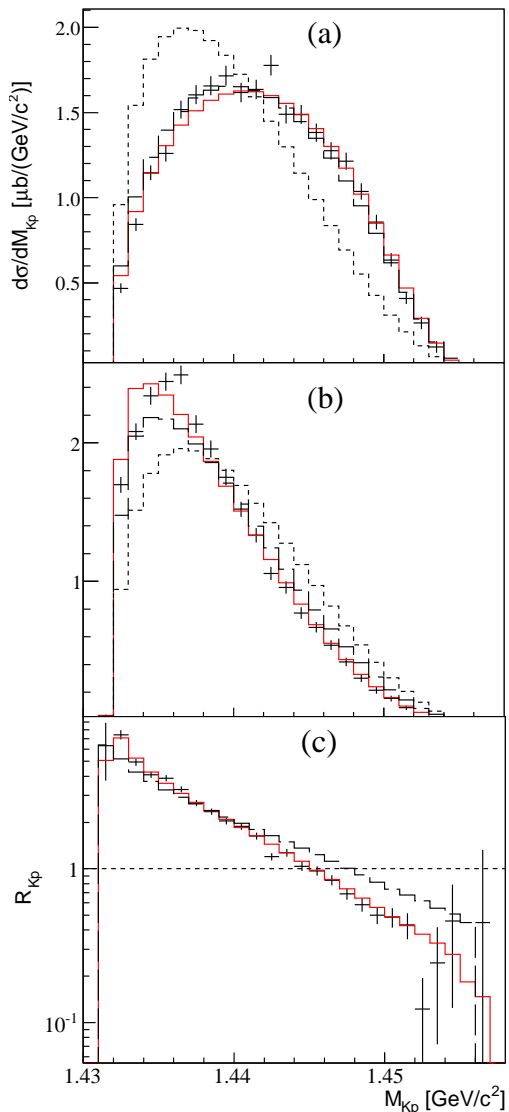


FIG. 5: (Color online) Differential cross sections for the  $pp \rightarrow ppK^+K^-$  reaction as functions of the invariant masses of  $K^+p$  (upper panel) and  $K^-p$  (middle panel), and their ratio  $R_{Kp}$  (lower panel). The red solid and dashed black histograms represent estimations based on Eq. (1) that take into account  $K^-p$ ,  $pp$  and  $K^+K^-$  final state interactions with  $a_{K^-p} = 2.45i$  fm and  $a_{K^+K^-} = 1.5i$  fm, respectively. The four-body phase-space simulations are shown by the dotted histograms.

in this region might also be influenced by  $K^-p \rightleftharpoons \bar{K}^0n$  channel coupling.

Due to the low statistics, the COSY-11 data at 10 and 28 MeV [4, 19] cannot distinguish between predictions based on effective scattering lengths of  $a_{K^-p} = 1.5i$  fm and  $a_{K^-p} = 2.45i$  fm. This is illustrated for the  $R_{Kp}$  ratio in Fig. 7 but this lack of sensitivity is equally true for  $R_{Kpp}$ .

The  $pp \rightarrow ppK^+K^-$  differential cross section, shown in Fig. 3 as a function of the  $K^+K^-$  invariant mass, was

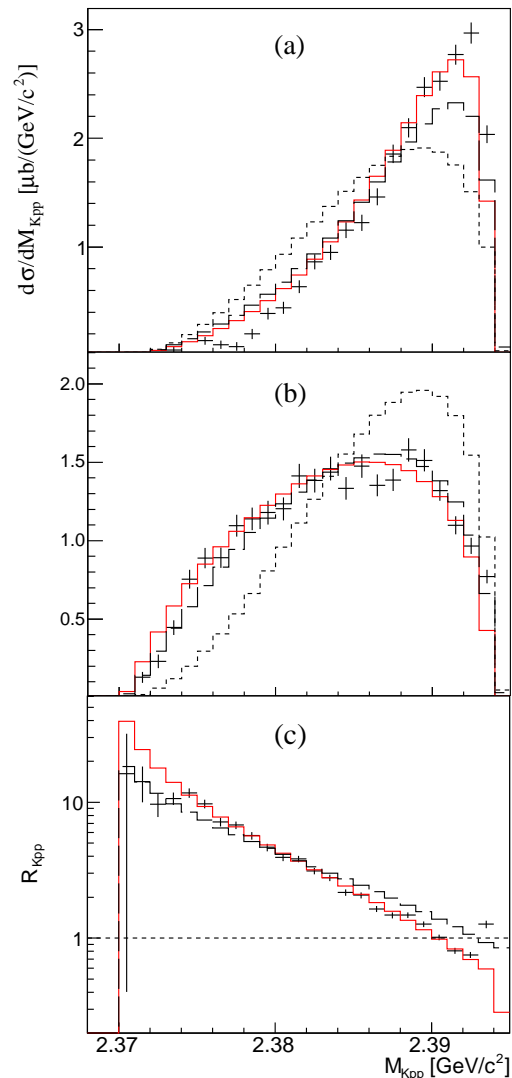


FIG. 6: (Color online) Differential cross sections for the  $pp \rightarrow ppK^+K^-$  reaction with respect to the invariant masses of  $K^+pp$  (upper panel) and  $K^-pp$  (middle panel), and their ratio  $R_{Kpp}$  (lower panel). The conventions for the theoretical estimates are as in Fig. 5.

used to determine the value of the total cross section,  $\sigma = 6.66 \pm 0.08 \pm 0.67$  nb, where the first error is statistical and the second systematic. The systematic effects considered here arise from the background subtraction, acceptance correction, tracking efficiency correction, and luminosity determination.

The total cross section result is plotted in Fig. 8 along with previous measurements from DISTO [5], COSY-11 [2–4, 19], and ANKE [6, 8]. The new point seems high compared to the COSY-11 result at  $\varepsilon = 28$  MeV, though one has to take into account the limited statistics of these data. This value had already been increased by 50% compared to that originally published [4]. This was achieved through a re-analysis of the data that in-

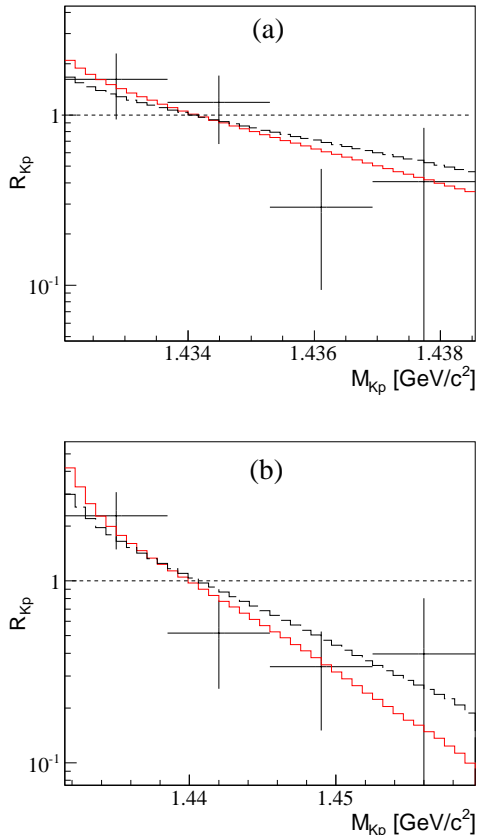


FIG. 7: (Color online) The ratio  $R_{Kp}$  for the  $pp \rightarrow ppK^+K^-$  reaction measured by COSY-11 at (a)  $\varepsilon = 10$  MeV and (b) 28 MeV [19]. The dotted histograms represent the four-body phase-space simulations, whereas the red solid and dashed ones represent the theoretical calculations taking into account  $K^-p$ ,  $pp$  and  $K^+K^-$  final state interactions with  $a_{K^-p} = 2.45i$  fm and  $1.5i$  fm, respectively.

cluded a modified  $pp$  and a  $K^-p$  final state interaction with  $a_{K^-p} = 1.5i$  fm [19]. For the lower excess energy of  $\varepsilon = 10$  MeV, where the acceptance of the COSY-11 apparatus is higher, the re-analysis increased the cross section by only 20%. Both cross sections would be reduced slightly if  $a_{K^-p}$  were increased to  $2.45i$  fm but the changes would be less than the statistical errors [20]. The COSY-11 acceptance is very sensitive to the form assumed for the  $pp$  FSI but much less so for that of the  $K^-p$  [20].

It is clear from Fig. 8 that the four-body phase space cannot reproduce the energy dependence of the total cross section. With the inclusion of the  $pp$ ,  $K^+K^-$ , and  $K^-p$  FSI, with an effective scattering length of  $a_{K^-p} = 1.5i$  fm, the data above the  $\phi$  threshold can be described well but those at lower energy are significantly underestimated. An increase in the value of  $a_{K^-p}$  might help in this region but the coincidence of strong effects in different two- or even three-body channels must

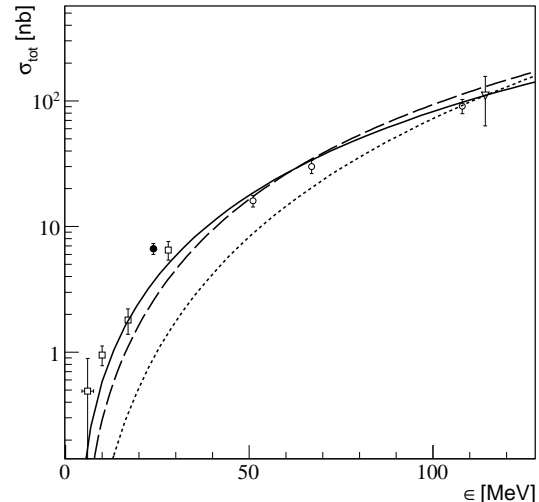


FIG. 8: Total cross section for the  $pp \rightarrow ppK^+K^-$  reaction as a function of excess energy  $\varepsilon$ . The present result (closed circle) is shown together with earlier experimental data taken from DISTO (triangle), ANKE (circles), COSY-11 (squares). The dotted line shows the four-body phase space simulation, whereas the solid line represent the simulations with  $a_{K^-p} = 1.5i$  fm. The predictions of a one-boson exchange model are represented by the dashed line [21].

also bring the factorization assumption of Eq. (1) into question. The dashed line, which represents a calculation within a one-boson exchange model [21], also underestimates the near-threshold data. This model includes energy-dependent input derived from fits to the  $K^\pm p \rightarrow K^\pm p$  total cross sections, though it does not include the  $pp$  final state interaction.

#### IV. DISCUSSION AND CONCLUSIONS

The production of  $K^+K^-$  pairs has been measured in the  $pp \rightarrow ppK^+K^-$  reaction channel at an excess energy of  $\varepsilon = 23.9$  MeV. Even taking its  $4.3$  MeV/ $c^2$  width into account, this is well below the central  $\phi$ -meson threshold at  $32.1$  MeV. The reaction was identified in ANKE through a triple coincidence of a  $K^+K^-$  pair and a forward-going proton, with an additional cut on the  $K^+K^-p$  missing-mass spectrum. The high statistics and low excess energy allow us to produce a detailed  $K^+K^-$  invariant mass distribution below the  $\phi$  threshold.

The distortion of both the  $K^-p$  and  $K^-pp$  spectra, which are even stronger than in our higher energy data, can be explained quantitatively within the product ansatz of Eq. (1) with an effective  $K^-p$  scattering length  $a_{K^-p} \approx 2.45i$  fm. This is to be compared with the  $1.5i$  fm obtained from the analysis of data measured above the  $\phi$  production threshold. A full treatment of the dynamics of the four-body  $ppK^+K^-$  channel is currently imprac-

tical. As a consequence, an energy dependence of  $a_{K^-p}$  is possible because this is merely an effective parameter within a very simplistic description of the four-body final state interaction. The strong  $K^-p$  final state interaction may be connected with the  $\Lambda(1405)$  in the production process and it has been suggested [11] that the production of non- $\phi$  kaon pairs proceeds mainly through the associated production  $pp \rightarrow K^+p\Lambda(1405)$ . This would also lead to deviations from the simple product ansatz for the final state interactions, not least because an attraction between the  $\Lambda(1405)$  and the proton would involve three final particles.

Our results show a very strong preference for low  $K^-pp$  masses and this effect seems to be even more marked than in the higher energy data [6, 8]. Although this might be connected with the ideas of a  $K^-pp$  deeply bound state [12, 22–24], it must be stressed that our data were measured far above threshold. They should not therefore be taken as necessarily implying that the  $K^-$  will bind with two protons.

There is strong evidence for a cusp effect arising from the  $K^0\bar{K}^0 \rightleftharpoons K^+K^-$  transitions. Our analysis within a coupled-channel description suggests that, with the values of the  $K\bar{K}$  scattering lengths used, the production of isospin-zero  $K\bar{K}$  pairs dominates. Though this is consistent with results extracted from data taken above the  $\phi$  threshold [7, 8], there is clearly room for some refine-

ment in the model. On the other hand, the structure of the  $K^-p$  invariant mass spectrum of Fig. 5 in the 1437 MeV/ $c^2$  region suggests that there might be important coupling also between the  $K^-p$  and  $K^0n$  systems.

It is evident that the interactions in the four-body  $ppK^+K^-$  final state are extremely complex. Nevertheless, the energy dependence of the total cross section can be well described above the  $\phi$  threshold by introducing the effects of the  $pp$ ,  $K^+K^-$  and  $K^-p$  final state interaction with an effective scattering length of  $a_{K^-p} = 1.5i$  fm. This would, however, have to be increased to have any hope of fitting the lower energy data. Further theoretical work is required to clarify the reaction mechanisms.

### Acknowledgments

We would like to thank the COSY machine crew for providing the good conditions that were necessary for this work. We are also grateful for the continued assistance of other members of the ANKE Collaboration. Discussions with P. Moskal and M. Silarski were very helpful. This work was supported in part by the US Department of Energy under Contract No. DE-FG02-03ER41231 and COSY FFE.

- 
- [1] W. Oelert, *Proceedings of the Workshop on Meson Production, Interaction, and Decay, Cracow, 1991*, Ed. A. Magiera, W. Oelert, and E. Grosse (World Scientific, Singapore, 1991) p. 199.
  - [2] M. Wolke, Ph.D. thesis, Westfälische Wilhelms-Universität Münster (1998).
  - [3] C. Quentmeier *et al.*, Phys. Lett. B **515**, 276 (2001).
  - [4] P. Winter *et al.*, Phys. Lett. B **635**, 23 (2006).
  - [5] F. Balestra *et al.*, Phys. Rev. C **63**, 024004 (2001).
  - [6] Y. Maeda *et al.*, Phys. Rev. C **77**, 015204 (2008).
  - [7] A. Dzyuba *et al.*, Phys. Lett. B **668**, 315 (2008).
  - [8] Q. J. Ye *et al.*, Phys. Rev. C **85**, 035211 (2012).
  - [9] C. Wilkin, Acta Phys. Polon. Suppl. **2**, 89 (2009).
  - [10] R. H. Dalitz and S. F. Tuan, Phys. Rev. Lett. **2**, 425 (1959).
  - [11] J. J. Xie and C. Wilkin, Phys. Rev. C **82**, 025210 (2010).
  - [12] T. Yamazaki *et al.*, Phys. Rev. Lett. **104**, 132502 (2010).
  - [13] R. Maier *et al.*, Nucl. Instrum. Meth. Phys. Res. A **390**, 1 (1997).
  - [14] S. Barsov *et al.*, Nucl. Instrum. Meth. Phys. Res. A **462**, 364 (2001).
  - [15] M. Hartmann *et al.*, Int. J. Mod. Phys. A **22**, 317 (2007).
  - [16] M. Hartmann *et al.*, Phys. Rev. Lett. **96**, 242301 (2006).
  - [17] M. Büscher *et al.*, Nucl. Instrum. Meth. Phys. Res. A **481**, 378 (2002).
  - [18] H. J. Stein *et al.*, Phys. Rev. ST Accel. Beams **11**, 052801 (2008).
  - [19] M. Silarski *et al.*, Phys. Rev. C **80**, 045202 (2009).
  - [20] M. Silarski and P. Moskal, private communication (2013).
  - [21] A. Sibirtsev, W. Cassing, and C. M. Ko, Z. Phys. A **358**, 101 (1997).
  - [22] M. Agnello *et al.*, Phys. Rev. Lett. **94**, 212303 (2005).
  - [23] T. Yamazaki and Y. Akaishi, Phys. Rev. C **76**, 045201 (2007).
  - [24] N.V. Shevchenko, A. Gal, J. Mareš, and J. Révai, Phys. Rev. C **76**, 044004 (2007).